

Scientific Paper

CLIMATE CHANGE AND CARBON FLUX IN THE BARENTS SEA: 3-D SIMULATIONS OF ICE-DISTRIBUTION, PRIMARY PRODUCTION AND VERTICAL EXPORT OF PARTICULATE ORGANIC CARBON

Dag SLAGSTAD and Paul WASSMANN*

*The Foundation of Scientific and Industrial Research (SINTEF), Division of Automatic Control,
The Norwegian Institute of Technology, N-7034 Trondheim-NTH, Norway*

Abstract: A 3-dimensional model is described that simulates current fields, ice-distribution, hydrography, primary production and vertical export of phytoplankton carbon in the Barents Sea. The model uses input data from meteorological stations and data from Det Norske Meteorologiske Institutt (MI) hindcast database. From initial fields of temperature and salinity, changes in the hydrography as a result of transport, fresh-water supply from land, cooling/heating and melting/freezing of ice is simulated. A warm year (1984) and a cold year (1981) were selected in order to investigate how the climate may effect primary production and vertical flux. The annual production of phytoplankton is in particular dependent on the ice distribution during spring. When the ice melts, strong vertical stability is created which reduces the vertical transport of nutrients compared to conditions where thermal heating alone creates stability. A maximal extent of ice-distribution gives thus rise to a maximum area of strong stratification after the ice-melt. Comparing the cold and warm year simulated here, primary production was up to 400% higher in the ice-free area during the warm year. The total annual primary production for the whole Barents Sea increased about 30% during the warm year. Even greater variations were discovered for the vertical flux of carbon.

1. Introduction

The Barents Sea is an arctic marginal shelf sea of the eastern North Atlantic which supports one of the richest fisheries of the world ocean. It is the western-most part of the extensive, wide and permanently or seasonally ice-covered shelf surrounding the Arctic Ocean on the Eurasian side. The two main water masses, Arctic water entering the Barents Sea from north-east and Atlantic water entering from south-west, are separated by the Polar Front. The Arctic water is periodically ice-covered and the maximum extension of ice is close to the Polar Front in the western and central part of the Barents Sea while ice-cover in the eastern part is more extensive (LOENG, 1991). The ice melts during spring and summer, giving rise to a stratified and nutrient rich euphotic zone which supports a distinct phytoplankton bloom in the marginal ice zone (SAKSHAUG and SKJOLDAL, 1989; WASSMANN and SLAGSTAD, 1993). In the areas dominated by Atlantic water stratification develops slowly by solar radiation solely during spring and summer and the resulting phytoplankton bloom is less distinct (SKJOLDAL and REY, 1989). The

* Norwegian College of Fishery Science, University of Tromsø, N-9037 Tromsø, Norway.

ice-coverage varies greatly from year to year, reflecting the interannual dynamics of inflowing Atlantic water (MIDTTUN and LOENG, 1987; ÅDLANDSVIK and LOENG, 1991) which is warm, nutrient rich and capable of introducing extensive, but variable amounts of zooplankton into the southern and central Barents Sea (SKJOLDAL and REY, 1989; TANDE, 1991; PEDERSEN, 1995). The dynamics of sea ice in the Barents Sea and its regulation of primary production during the short productive period at latitudes north of 70°N are, therefore, capable of influencing the carbon flux dynamics of the area, both seasonally and inter-annually. Climatic forcing is supposed to play a significant role for the carbon flux in the Barents Sea.

The data sets gathered by the Norwegian Research Program of Marine Arctic Ecology (PRO MARE) and other investigations during the years 1979–1989 are too small to address adequately the annual or inter-annual dynamics of carbon flux of a large shelf area like the Barents Sea (for overviews, see LOENG, 1987 and SAKSHAUG *et al.*, 1991). However, understanding the large-scale dynamics of carbon flux in the Barents Sea is nonetheless crucial for understanding the functioning of this ecosystem. Among many examples we present 2 fields of interest where such knowledge is of importance.

(a) The Barents Sea supports one of the largest fisheries in the world and changes in fish stocks are of great concern to fishermen and authorities alike. Variations in fish stocks are connected to variations in new and secondary production (LEGENDRE, 1990; IVERSON, 1990) as well as the total primary production in the region supporting fish stocks (SKJOLDAL and REY, 1989). In addition, advection of meso-zooplankton along with the influx of Atlantic water into the southern and central Barents Sea can introduce food for capelin, the key pelagic fish species in the Barents Sea. Advection of meso-zooplankton can be of the same order of magnitude as endemic growth (PEDERSEN, 1995). The influx of Atlantic water is variable and controlled by meteorological forces (ÅDLANDSVIK and LOENG, 1991).

(b) Recent models of the ocean-atmosphere system demonstrate the potentially great importance of polar seas to the regulation of atmospheric CO₂. This is due, in great part, to the action of the surface biota. Polar seas have a large influence on the atmosphere's CO₂ content (BROECKER and PENG, 1990; ANDERSON *et al.*, 1990) compared to other areas of the world's ocean, mainly due to deep-water formation. For arctic waters to be a true sink of atmospheric CO₂ a large proportion of the fixed carbon must become inaccessible to the atmosphere (SARMIENTO and TOGGWEILER, 1984). One way this can happen is if carbon fixed by photosynthesis sinks to intermediate depths in particulate form. This loss of organic matter from surface waters takes place through settling of phytoplankton cells, faecal pellet production by zooplankton and plankton-derived detritus.

In a remote area like the Barents Sea, the only adequate method to address the question of climate change and carbon flux at present seems to be mathematical modelling based on information available on the physical, chemical and biological oceanography of the area. Several modelling attempts regarding the Barents Sea have been presented in the literature (*e.g.* SLAGSTAD and STØLE-HANSEN, 1991; STØLE-HANSEN and SLAGSTAD, 1991; WASSMANN and SLAGSTAD, 1993). Unfortunately, data to prove the results of the models are scarce or often not existing. For example, the hydrography in the eastern and northern part under the ice cover, during winter as well as vertical mixing is inadequately known. The dynamics of zooplankton in the eastern part of the Barents

Sea are supposed to be different compared to the central and northern part (K. TANDE, pers. commun.), but sufficient data are lacking. Only a few measurements of primary production (REY *et al.*, 1987) and vertical flux (WASSMANN *et al.*, 1991) have been carried out in the central Barents Sea. The possibility of numerous inaccurate representation of the driving forces in the model open the door for inaccurate results after some time of simulation, without the possibility of being updated to reality.

The present simulation results are some first approximations apt to investigate the variability of particulate carbon flux in the Barents Sea as a function of climate change. For this reason, a cold year (1981) and a warm year (1984) were selected and modelled in order to illustrate the climatic dynamics of the carbon flux in the Barents Sea. Nevertheless, this contribution represents just another step addressing quantitatively the dynamics of primary and vertical flux of the entire Barents Sea until more extensive data sets are available.

2. Description of the Model

The model is a 3-dimensional, baroclinic, finite difference “level model” which is defined with a sequence of fixed, but penetrable levels. Each level has a fixed thickness, with the exception of the level at the surface and the one which by chance is close to the bottom. The number of levels will thus be a function of the horizontal co-ordinates.

2.1. Basic equations

Taking horizontal and vertical turbulent diffusion of momentum into consideration, equations which describe movement of an incompressible fluid on a rotating base can be described in the following way:

Acceleration in the x -direction:

$$\frac{\partial u}{\partial t} = fv - u \frac{\partial u}{\partial x} - v \frac{\partial u}{\partial y} - w \frac{\partial u}{\partial z} - \frac{1}{\rho} \frac{\partial p}{\partial x} + A_v \nabla^2 u + \frac{\partial}{\partial z} A_v \frac{\partial u}{\partial z} \quad (1)$$

Acceleration in the y -direction:

$$\frac{\partial v}{\partial t} = -fu - u \frac{\partial v}{\partial x} - v \frac{\partial v}{\partial y} - w \frac{\partial v}{\partial z} - \frac{1}{\rho} \frac{\partial p}{\partial y} + A_v \nabla^2 v + \frac{\partial}{\partial z} A_v \frac{\partial v}{\partial z} \quad (2)$$

The vertical velocity (w) is deviated from the continuity equation:

$$\frac{\partial w}{\partial z} + \frac{\partial u}{\partial x} + \frac{\partial v}{\partial y} = 0, \quad (3)$$

and the surface elevation (η) from:

$$\eta = \int w_1 dt, \quad (4)$$

where

- u, v - horizontal velocity components in the x and y direction,
- w_1 - vertical velocity of the surface level,

- η - height of the free surface relative to an undisturbed average value,
 f - Coriolis parameter,
 ρ - density,
 A_h - horizontal turbulent diffusion of momentum,
 A_v - vertical turbulent diffusion of momentum,
 p - pressure, calculated from the hydrostatic equation:

$$p(z) = \int_z^\eta \rho g dz + Pa, \quad (5)$$

where Pa is the atmospheric pressure.

The variation of the density in space and time is calculated from equation of state

$$\rho = \rho(S, T), \quad (6)$$

where S and T are salinity and temperature. These scalar fields can be modelled with the balance equation

$$\frac{\partial c}{\partial t} = -\frac{\partial}{\partial x}(uc) - \frac{\partial}{\partial y}(vc) - \frac{\partial}{\partial z}(wc) + K_h \nabla^2 c + \frac{\partial}{\partial z} \left(K_v \frac{\partial c}{\partial z} \right) + \delta_c, \quad (7)$$

where

- c - S or T ,
 K_h - horizontal turbulent diffusion of salinity and temperature,
 K_v - vertical turbulent diffusion of salinity and temperature,
 δ_c - $c=T$: heat flux through the sea surface,
 $c=S$: supply of fresh water or freezing/melting of ice,

and the operator ∇^2 means,

$$\nabla^2 \Theta = \frac{\partial^2 \Theta}{\partial x^2} + \frac{\partial^2 \Theta}{\partial y^2}, \quad (8)$$

where Θ is a function of x and y .

2.2. Vertical mixing

The vertical turbulent mixing coefficient, A_v , is calculated as a function of the Richardson number (R_i) and the state of the sea surface (waves). The Richardson number

$$R_i = \frac{g \frac{\partial \rho}{\partial z}}{\rho \left(\left(\frac{\partial u}{\partial z} \right)^2 + \left(\frac{\partial v}{\partial z} \right)^2 \right)}, \quad (9)$$

is large if the water column is stable and decreases if the vertical density gradient decreases and if the vertical mixing increases. According to PRICE and WELLER (1986) the current becomes turbulent if R_i becomes smaller than about 0.65. Cooling of the surface can produce denser water, giving rise to convection. This is simulated as a instantaneous

mixing with a indefinitely high mixing coefficient. The equation which is used to calculate the vertical mixing coefficients is

$$A_v(\rho, u, v, W, z) = A_{vm} \left\{ \operatorname{atan} \frac{k(R_{i0} - R_i) + 0.5}{\pi} \right\} + a_w(W, z) + a_{\text{tide}}, \quad (10)$$

where A_{vm} is the maximum vertical diffusion, *i.e.* the asymptotic value of A_v when R_i approaches minus infinity, R_{i0} is the value of the Richardson number where the current changes from laminar to turbulent and k is a parameter which indicates how rapidly the vertical diffusion changes when the Richardson number is close to R_{i0} . $a_w(W, z)$ is a function describing the vertical, turbulent diffusion as a function of the wave height and wave period which in turn is a function of wind speed (ICHIYE, 1967).

$$a_w(W, z) = 0.028 \frac{H^2}{T} e^{-2kz}, \quad (11)$$

where H is the wave height, T is the average wave period, k is the wave number. H and T are related to wind by an empirical equation from the JONSWAP programme (HASSELMANN *et al.*, 1973). If the fetch length is 500 km, $H=0.4 W$ and $T = 3.6 W^{0.33}$, and W is the wind speed.

The wave number is found from a dispersion equation, $\omega^2 = gk$, where $\omega = 2\pi/T$. a_{tide} depends on the local magnitude of the currents and depth. It is calculated from an equation by LODER and GREENBERG (1986):

$$\log \left(\frac{h}{\rho C_D |\mathbf{v}|^3} \right) \leq 2.9, \quad (12)$$

where h is the depth, ρ is water density, C_D is bottom drag coefficient and \mathbf{v} is the velocity vector. When the condition of eq. (12) is valid, it is assumed that the mixing coefficient is so high that the water column is completely mixed. Only M_2 is used to calculate the tide component. In the model area in this publication (see Fig. 2) only the Svalbard bank and shallow areas north of Russia tidal mixing will be of significance. Parameters used in the model are $A_{vm} = 0.03 \text{ m}^{-2} \text{ s}^{-1}$, $R_{i0} = 0.65$, $k = 30$.

2.3. Ice model

If a model is supposed to simulate the carbon flux in the central and northern Barents Sea, it must have a representation of the ice coverage. This is due to physical as well as due to biological reasons. Ice influences the vertical stability of the water column both during melting and freezing. During freezing salt is discharged from the ice, heavy water is produced and mixed with upper water. Smelting gives rise to almost freshwater. This water creates a less dense surface layer and intense stratification. The ice cover will further act like a shield obstructing radiation. Ice functions as an isolator, reducing the flux of heat from the sea to the atmosphere. Knowing the temperature profile of the water column and some meteorological variables (air temperature, humidity, cloud cover and radiation) the growth of sea ice could be calculated with great precision. However, in the open ocean wakes and polynias will be formed due to the movement of the ice which makes modelling of the growth of sea ice much more difficult. The expanse of sea ice is variable and thick and thin areas of sea ice can be found simultaneously in the

same area. Sea ice is plastic during convergence, but breaks easily into pieces during divergence, giving rise to wakes. These wakes have a significant loss of heat and a thin ice cover is often formed. During convergence thin ice is pressed into thick ridges. Complicated ice models (HIBLER, 1979) are based on the thickness of the ice cover in order to calculate the heat loss. The model presented here is similar to that of HIBLER (1979) and has two variables: ice thickness (h) and ice compactness (A). In every horizontal grid cell (here 20×20 km) h will have an average thickness and A represents that part of the cell which is covered by thick ice. The rest of the cell is covered by thin ice is assumed to have 0 thickness, *i.e.* open water. Open water represents therefore a combined fraction of water and thin ice up to a thickness of h_0 (which will be explained later). The remaining distribution of ice is randomly distributed. The amount of thin ice is, however, small compared to the thick fraction and it is assumed that the thick ice fraction has the thickness h/A . For intermediate ice thickness the following equation is used:

$$\frac{\partial h}{\partial t} = - \frac{\partial(u_{\text{ice}}h)}{\partial x} - \frac{\partial(v_{\text{ice}}h)}{\partial y} + S_h, \quad (13)$$

$$\frac{\partial A}{\partial t} = - \frac{\partial(u_{\text{ice}}A)}{\partial x} - \frac{\partial(v_{\text{ice}}A)}{\partial y} + S_A, \quad (14)$$

where u_{ice} and v_{ice} are the horizontal velocity components of the ice. Since A represents the relative coverage of the area it is required that $A \leq 1$. S_h and S_A are thermodynamic equations:

$$S_h = f(h/A) A + (1-A) f(0), \quad (15)$$

$$S_A = \begin{cases} (f(0)/h_0) (1 - A), & \text{if } f(0) > 0 \\ 0, & \text{if } f(0) < 0 \end{cases} \quad (16)$$

$$+ \begin{cases} 0, & \text{if } S_h < 0 \\ (A/2h) S_h, & \text{if } S_h > 0, \end{cases}$$

$f(h)$ is the growth velocity of the ice with a thickness of h . S_h is given as a sum of the net ice index or melting in open water and that part of the grid cell which is covered by ice, respectively.

S_A characterises the mutual effect between thin ice and the thick ice in a grid cell. The first part of eq. (16) is a parameterization of that movements in the ice compress the thin ice with the result that a thickness h_0 is achieved and thus the area of with thick ice increases. h_0 is in the simulations 0.5 m. The second part of the equation takes into consideration that melting will reduce the area covered by ice by a gradual removal of the thinnest ice. It is assumed that the ice thickness is uniformly distributed with a thickness between 0 and $2 h/A$. During the time step Δt all ice with the thickness $-S_h \Delta t$ is removed and the relative area with open water will increase. The drifting velocity of the ice is given by 2.5% of the wind speed with a 10° direction to the right (ZUBOV, 1945; LØYNING and VINJE, 1991) plus the velocity of the underlying water.

2.4. Numeric calculation scheme and boundary conditions

The equations for movement of mass and continuity are solved with a finite difference method comparable to that described by TINGELE *et al.* (1979). The state variables are discretized in space and with a staggered grid, also known as Arakawa C grid (MESINGER and ARAKAWA, 1976). Central difference is used for the integration in space, while a two-level, semi-implicit scheme is used for the integration of time. A hybrid scheme where central and upstream differences are combined integrate the non-linear components. Advection of temperature and salt was approximated by a second order upstream scheme. Details regarding the numerical methods used in the model can be found in SLAGSTAD (1987), SLAGSTAD *et al.* (1989) and STØLE-HANSEN *et al.* (1989). The so-called flow relaxation scheme (FRS) was used at the open boundaries (MARTINSEN and ENGEDAHL, 1987).

2.5. Phytoplankton model

Transport and distribution of a scalar entity such as phytoplankton (P) or nitrogen (N) is governed by eq. (7). Velocities and vertical mixing coefficients are taken from the hydrodynamical model. In the Barents Sea, ice is important for the light conditions in the water column. Ice cover is modelled by a ice model. The equations describing the growth of phytoplankton at a certain depth are:

$$\frac{dP}{dt} = PP_m^B \frac{\text{Chl}}{C} \left[\min \left\{ 1 - \exp \left(\frac{-\alpha^B I_z}{P_m^B} \right), \frac{N}{k_N + N} \right\} \right] - Pr - PS_{\text{sed}}, \quad (17)$$

$$\frac{dN}{dt} = -PP_m^B \frac{\text{Chl}}{C} \left[\min \left\{ 1 - \exp \left(\frac{-\alpha^B I_z}{P_m^B} \right), \frac{N}{k_N + N} \right\} \right] + 0.5 Pr, \quad (18)$$

where P_m^B [mg C (mg Chl)⁻¹h⁻¹] is the maximum photosynthetic rate, Chl/C is the chlorophyll *a*: carbon ratio, α^B [mg C (mg Chl)⁻¹h⁻¹ ($\mu\text{mol m}^{-2}\text{s}^{-1}$)⁻¹] is the Chlorophyll-*a* specific photosynthetic efficiency, k_N [mol N m⁻³] is the half saturation constant for uptake of nitrogen, r [h⁻¹] is the respiration rate, I_z is the irradiance at depth z , and S_{sed} [h⁻¹] is the sedimentation rate given by

$$S_{\text{sed}} = d_{\text{mn}} + (d_{\text{mx}} - d_{\text{mn}}) \exp \left\{ - \frac{N}{(k_N + N) / dg} \right\}, \quad (19)$$

where d_{mn} [h⁻¹] is the sedimentation rate when the concentration of nitrogen is high, d_{mx} [h⁻¹] is maximum sedimentation rate when the nutrient concentration is low and dg is a parameter which determined the functional relationship between sedimentation rate and concentration of nutrients. Grazing is simulated by a elevated respiration rate. Half of the losses from respiration/grazing is assumed to be regenerated whereas half is assumed to be exported out of the euphotic zone.

The photosynthetic available irradiance (PAR) is calculated from the local height of the sun after a model by BIRD (1983). Daily average cloud cover is interpolated from available meteorological stations in the Barents Sea. The depth variation of the irradiance is calculated after an equation of KIRK (1983):

Table 1. Parameters used in the phytoplankton model. *

Symbol	Value	Unit	Meaning
P_m^B	0.9	mg C (mg Chla) ⁻¹ h ⁻¹	Maximum photosynthetic rate
$\frac{\text{Chla}}{\text{C}}$	0.035	–	Chlorophyll-a : Carbon-ratio
α^B	0.02	mg C (mg Chla) ⁻¹ h ⁻¹ ($\mu\text{mol m}^{-2} \text{s}^{-1}$) ⁻¹	Photosynthesis per light unit
k_N	0.4	$\mu\text{mol N l}^{-1}$	Half saturation constant for uptake of nitrate
r	0.1	d ⁻¹	Respiration and grazing rate per unit biomass
d_{mn}	0.0004	h ⁻¹	Conversion rate from phytoplankton to “sinking phytoplankton” when the nitrate concentration is high
d_{mx}	0.00	h ⁻¹	Conversion rate from phytoplankton to “sinking phytoplankton” when the nitrate concentration is low
dg	0.1	–	Parameter
k_w	0.05	m ⁻¹	Attenuation coefficient for pure water
COSI	0.75	–	Average cosine for light in water

* Most of the parameters are taken from SAKSHAUG *et al.* (1991).

$$I_z = \frac{I_0}{\text{COSI}} \exp \left\{ \int_z^0 \frac{1}{\text{COSI}} (k_w + f_{\text{att}}(\text{Chl})) d\tau \right\}, \quad (20)$$

where, I_0 is the irradiance at the surface, k_w is the attenuation coefficient of pure sea water, COSI is the average cosine of light in water and $f_{\text{att}}(\text{Chl})$ is a function that calculates the attenuation due to chlorophyll in the water column (PARSONS *et al.*, 1983):

$$f_{\text{att}} = 0.0088Kl_0 + 0.054\text{Chl}^{2/3}. \quad (21)$$

For more information, see SLAGSTAD and STOKKE (1994) and SAKSHAUG *et al.* (1995).

The parameters used are given in Table 1.

2.6. Model configuration and driving forces

The model area is shown in Fig. 1. The depth of the levels from the surface is 10, 5, 5, 5, 5, 5, 10, 25, 25, 25, 25, 25, 25, 50, 100, 200, 400 and 1000 m, *i.e.* 20 layers covering up to 2000 m depth. The horizontal grid point distance is 20 km. The number of horizontal grid points is $150 \times 120 = 18000$.

The annual inflow of Atlantic water into the Norwegian, Icelandic and Greenland

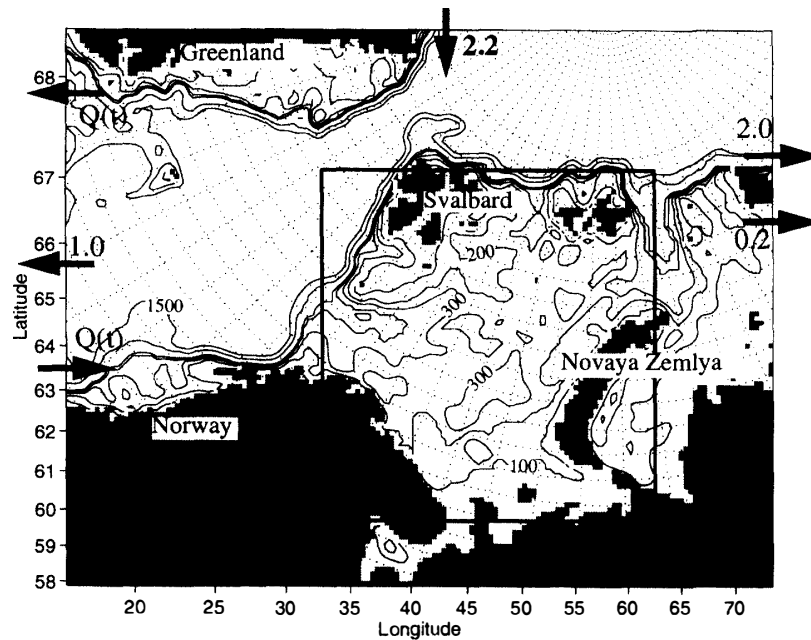


Fig. 1. The model area. The units on the axes are grid points where the lower left corner is grid point number 1,1. Since the distance between the grid points is 20 km, grid point number 100 is a distance of 2000 km from the lower left corner. Also shown is the flux of water through the open boundaries in Sverdrup ($10^6 \text{ m}^3 \text{ s}^{-1}$). Isobaths are shown for 100, 200, 300, 400, 500, 1000 and 1500 m. The square box indicates the area from where simulation data will be presented.

Sea based on heat budgets was calculated by WORTHINGTON (1970) to approximately 8 Sv. Comparable estimates were presented by MYSAK and SCHOTT (1977) and GOULD *et al.* (1985). The monthly average estimates can however vary between 4 and 12 Sv (GOULD *et al.*, 1985; McCLIMANS, 1993). In the simulation presented here a variable inflow of Atlantic water along the coast of mid Norway (Møre) which varies according to McCLIMANS (1993). The minimum in spring is 4 Sv and the maximum in December is 12 Sv. Outflow from the model area takes mainly place through the East-Greenland Current. The flux through of water the open boundaries of the model area are presented in Fig. 1.

The initial density field is based on the Levitus world database for temperature and salinity, but improved by the Institute of Marine Research in Bergen with data from autumn 1980 and 1983. Wind and the atmospheric pressure was taken from the The Norwegian Institute of Meteorology's (MI) hindcast database. These data are available on a 75 km grid and interpolation of these data to the model grid was necessary. The area east of Novaya Zemlya is not covered by the MI database and thus it has been necessary to extrapolate wind and air pressure. In order to calculate the heat flux, air temperature, humidity, cloud cover from meteorological stations within the model area are used. The coverage along the coast is relatively good. Russian data were unfortunately not available. We have, therefore, based on climatological atlas and educated guesses postulated the climatic development on Franz Josef Land, Novaya Zemlya and on the Kola peninsula. Based on these point measurements of the meteorological variables horizontal fields

covering the model area were interpolated.

3. Simulation Results and Discussion

The results which are presented here are a part of the model area (Fig. 1) and comprise primarily the Barents Sea. The connection between geographical position and grid point number is presented in Fig. 2. The left hand figure shows the position of "Transect I", one of the best investigated transects in the Barents Sea. Data from measurements will not be presented, but various sources can be applied (*e.g.* SKJOLDAL *et al.*, 1987; BÅMSTEDT *et al.*, 1991; WASSMANN *et al.*, 1991).

3.1. Current field

The current field changes rapidly along with the meteorological conditions and a good description of the current system as simulated by the model would demand significant expense. Only two examples of monthly averaged surface current fields in June 1981 and 1984 are shown in order to illustrate some of the physical driving forces behind the simulations of carbon flux presented below (Fig. 3). Many strong branches with currents are visible. The inflow of Atlantic water south of Bear Island is relatively strong and continues as a relatively narrow current into the Hopen Depth. There it splits up into a branch which goes to the east between the two banks Central Bank (south) and Great Bank (north), while the other branch goes northwards between Great Bank and Svalbard Bank. The flow pattern has previously been described by several models (*e.g.* McCLIMANS and NILSEN, 1990; HARMS, 1994). The simulation of the cold, south-going current east of Spitsbergen is weak. The current is density driven and with a grid point distance of 20 km it is difficult to keep the necessary density gradient driving the current.

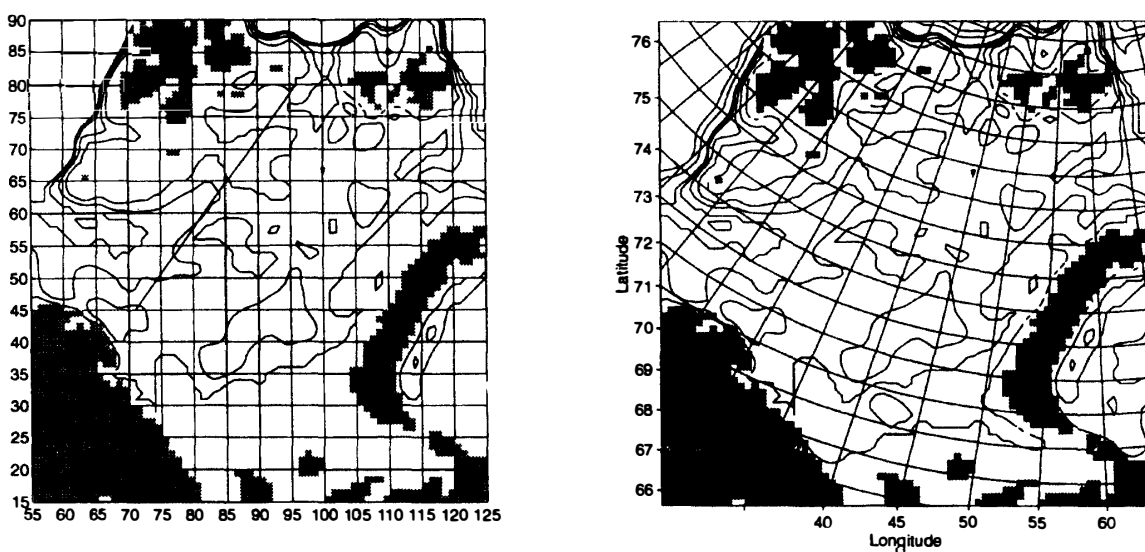


Fig. 2. The connection between the geographical position and the grid point number. The left figure shows the position of "Transect I". Isobaths on the right figure are shown at 100, 200, 300, 400, 500, 1000 and 1500 m.

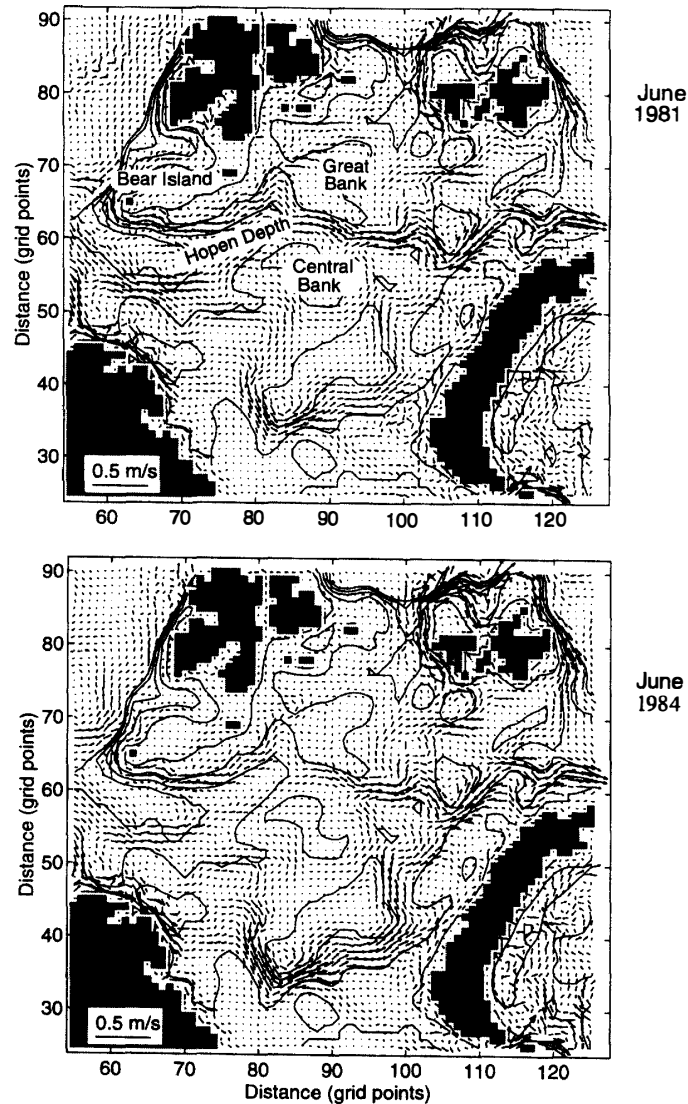


Fig. 3. Average surface current for June of the cold year 1981 (above) and the warm year 1984 (below), respectively.

The present model simulates the flow pattern and the current velocities in the Barents Sea sufficiently well as compared by verification with the available data. In general the differences in the flow pattern and the current velocities of the surface water in June are small between cold and warm years. Over the whole year, however, and over the whole water column significant differences are found between cold and warm years (data not shown).

3.2. Ice distribution

Simulated ice distribution and surface temperature belong to the variables which are most easily comparable with measurements. Figure 4 displays the simulated ice distribution at selected dates for cold (1981) and warm (1984) years. As an initial condition of the ice coverage a thickness of 2 m was assumed in the north and east of a line

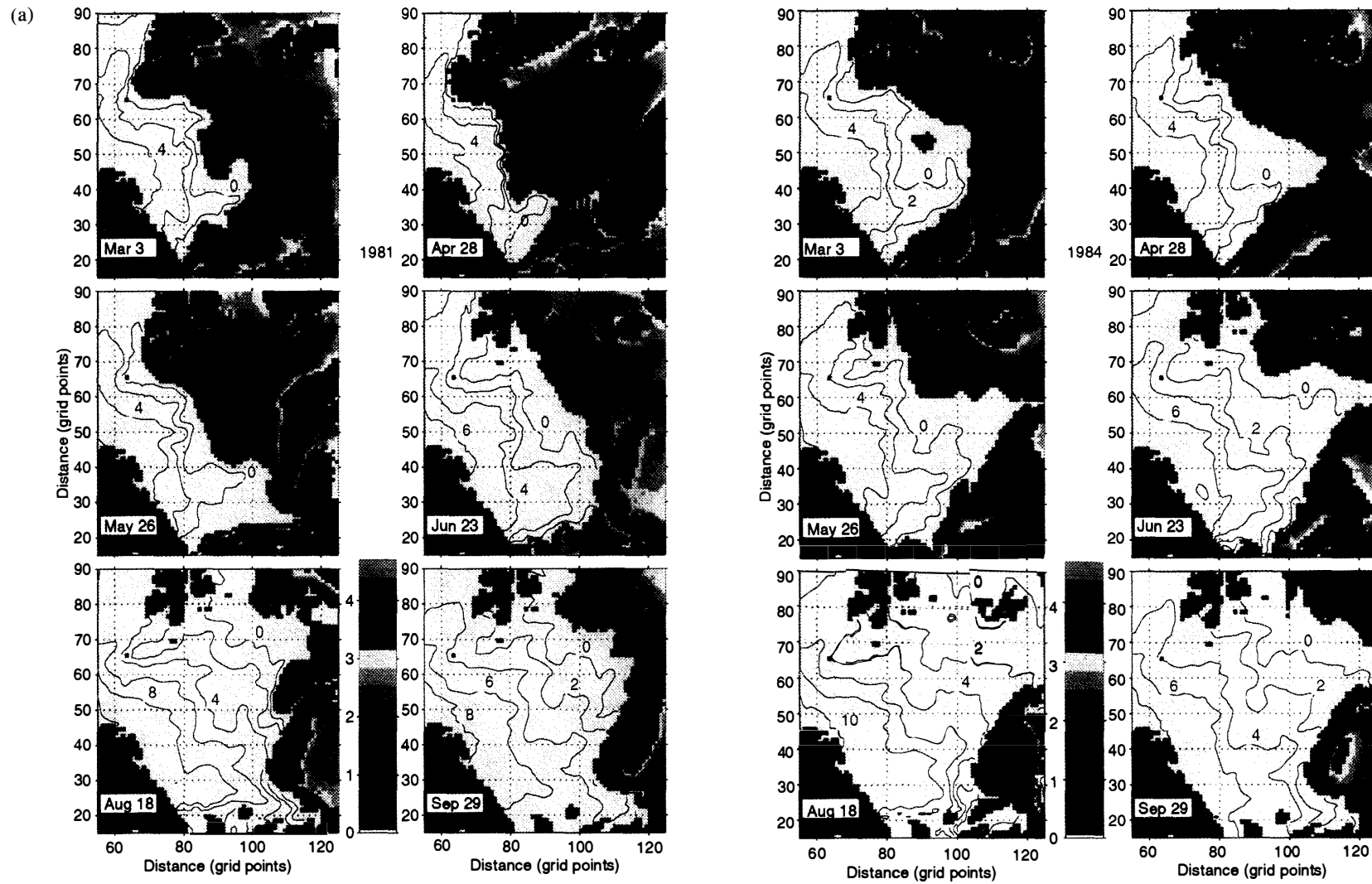


Fig. 4. Simulated ice distribution (shown as average ice thickness in m) and the sea surface temperature at selected dates between March and September 1981 (left) and 1984 (right). Isotherms for temperature are shown for every 2°C. The connection between the geographical position and the grid point number is found in Fig. 3.

stretching from Spitsbergen–Franz Joseph Land–Novaya Zemlya. The simulation for the cold year was started in October 1980. During the autumn and early winter the complete northern Barents Sea, along Novaya Zemlya and the shallow areas in the south-eastern Barents Sea were covered with ice. The predominant wind direction from the north and north-east resulted in a movement of ice to the south and west in March and April. The maximum ice distribution was found at the end of April and this is confirmed by ice distribution maps and satellite data. The withdrawal of the ice was rapid along the Kola Peninsula–Novaya Zemlya section. This was probably caused by the warm, east-bound current of Atlantic water which followed along the southern border of the south-eastern Barents Sea. The ice-free areas at Franz Joseph Land and Novaya Zemlya were noteworthy (*e.g.* Apr. 28 in Fig. 4a). Northerly winds will pack the ice north of the islands while at the southern and western shores the ice thickness is decreasing and even polynias were formed. This phenomenon is verified by satellite pictures (VINJE and KVAMBEKK, 1991). East of Spitsbergen, the simulated melting of ice during summer was somewhat greater than observed.

A comparison of the simulated ice distribution of the warm year 1984 with that of the cold year 1981 indicates the significant inter-annual differences in ice coverage in the Barents Sea (Fig. 4). The ice distribution during warm years is much smaller. This is caused by several reasons: (a) the heat content in the Barents Sea at the start of the simulation for 1984 (October 1983) was greater, (b) the ice distribution at the start of the simulation was smaller compared with 1981 and (c) reduced ice coverage during the previous year resulted in greater convection of heat to deeper layers. In the south-eastern part of the Barents Sea the amount of ice was far greater than observed during 1984. This suggests that the air temperature on the Kola Peninsula was set too low during this year. As mentioned earlier, meteorological data from Russia were not available and the condition in this part of the model area had to be guessed. The simulated ice coverage in the Kara Sea was greater than observed in 1984 which also suggests that the air temperature was put too low. In general, the model simulates well the ice dynamics in the Barents Sea for both warm and cold years. The simulations also suggest that the quality of the model is sufficient to model the ice distribution if the access to meteorological data is adequate.

3.3. Seasonal variation in phytoplankton biomass

The simulations of phytoplankton were started on March 1 and forced by the physical model. Among the physical factors and processes playing a role for the phytoplankton simulations are daily averaged current velocities in three dimensions, vertical mixing, temperature and ice coverage and concentration. The starting concentration of the phytoplankton and nitrate was $0.2 \text{ mg Chl m}^{-3}$ and 11 mmol N m^{-3} over the complete model area.

The simulated surface concentration of phytoplankton for the cold year 1981 is shown in Fig. 5. At the end of April there was an increase in the melt water zone around the ice edge. At the beginning of May phytoplankton production increased rapidly, in particular along the melt water areas between Norway and Novaya Zemlya. During May rapid phytoplankton growth was also recorded in other areas which had reached sufficient stability due to fresh water supply, for example the coast of Norway. At the

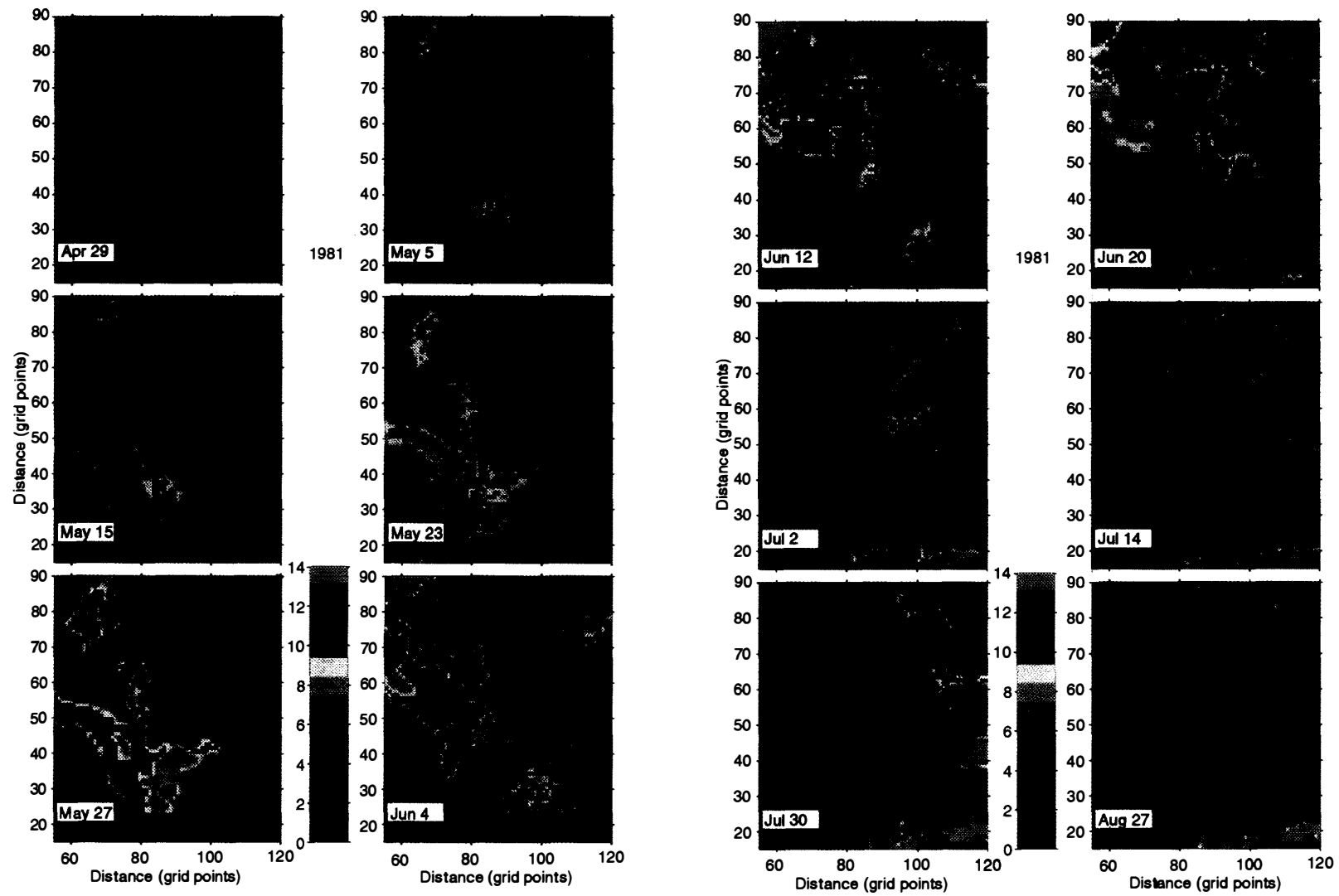


Fig. 5. Simulated concentration of chlorophyll (mg Chl m^{-3}) at the surface at selected dates during spring and summer 1981. The figure continues on the next page.

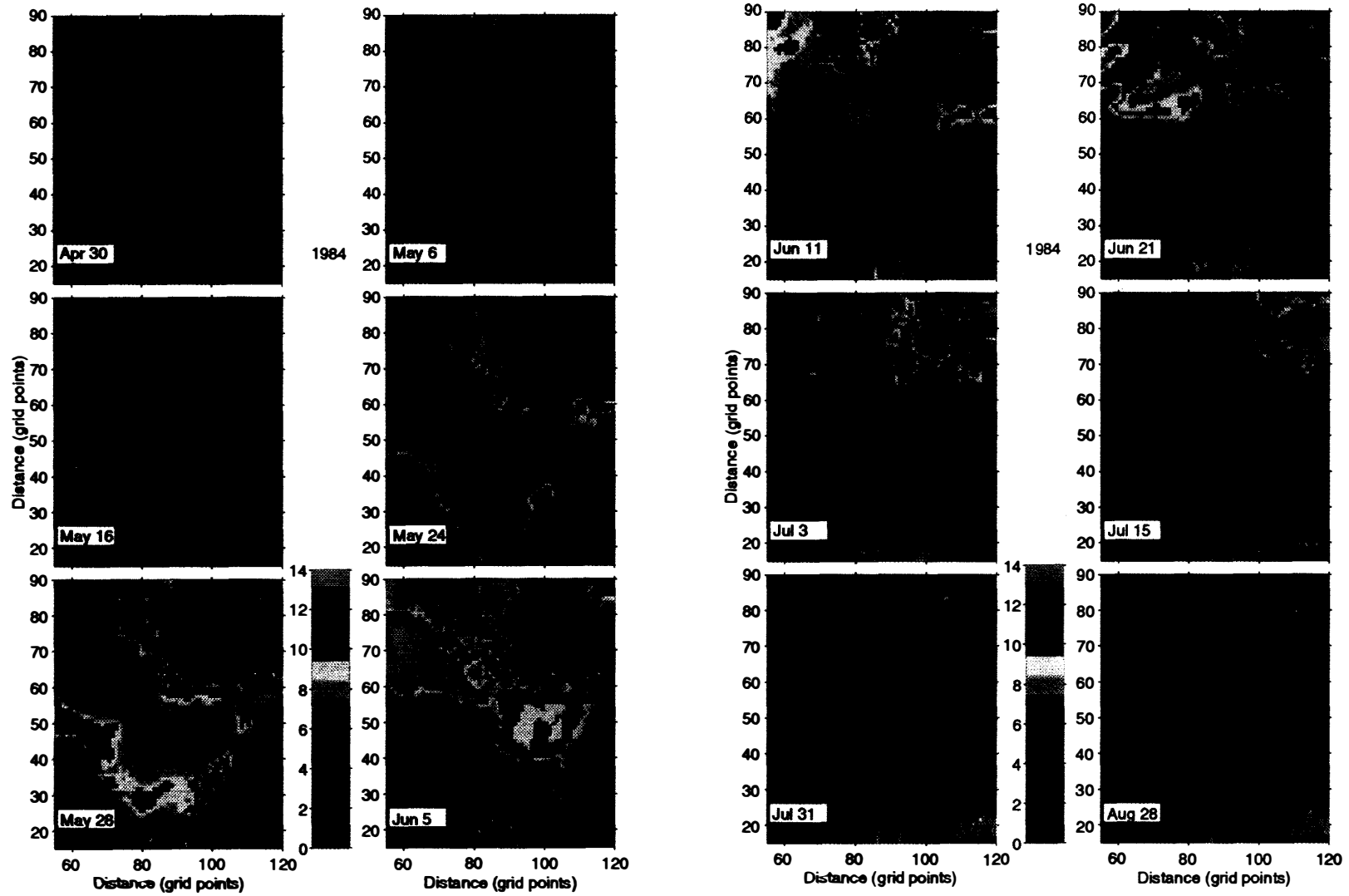


Fig. 6. Simulated concentration of chlorophyll (mg Chl m^{-3}) at the surface at selected dates during spring and summer 1984.

end of May phytoplankton bloom are found in all ice-free areas, with a small delay south of Bear Island. At the beginning of June the phytoplankton bloom had more or less come to an end in the surface water, with the exception of the marginal ice zone and in the Atlantic water in the western parts of the Barents Sea.

East of Spitsbergen the simulations show a phytoplankton bloom which started in the beginning of June and which stretched over time a long way behind the ice edge. A closer investigation revealed that the simulated ice concentration was low (40–60% ice coverage) and this resulted in sufficient light in the water column for phytoplankton growth. Ice data from MI revealed that this was actually the case.

The advance of the ice during March and April resulted in large areas with a brackish surface layer with increased vertical stability when the ice withdrew. Phytoplankton growth started immediately when radiation in the water column was sufficient. The simulated chlorophyll concentration often increased to 13 mg Chl m^{-3} . After the depletion of nutrients, part of the bloom sank from the surface layer into deeper water (see below). A chlorophyll maximum layer with concentration of about 14 mg Chl m^{-3} developed during summer.

The phytoplankton production in the warm year 1984 started a little later compared to the cold year 1981 (Fig. 6). This is due to less fresh water supply from melting ice and thus lower vertical stability. In the beginning of May the chlorophyll concentration increased in particular along the ice edge. The phytoplankton bloom in eastern part of the Barents Sea started again earlier than in the remaining areas. The development south of Bear Island was delayed compared to the other areas and the maximum biomass was first reached in early June. In the northern Barents Sea the phytoplankton production followed more or less the ice edge. Some of the increased phytoplankton concentrations close to the surface were caused by low pressure passages which eroded the pycnocline some meters lower into the water column, giving rise to increased flux of nutrients into the water column (SAKSHAUG *et al.*, 1995). At the end of July the ice had disappeared from the model area and only low chlorophyll concentrations were found in the surface layer, lasting for the rest of the summer.

3.4. Interannual carbon flux variation and climatic forcing

The total primary production of the warm year 1984 was clearly higher compared to the cold year 1981 (Fig. 7). The highest production ($80\text{--}100 \text{ g C m}^{-2} \text{ y}^{-1}$) was found around Bear Island, the Bear Island Bank, Spitsbergen and south-east of Novaja Zemlja. The basic patterns in primary production are also reflected in vertical carbon flux (Fig. 7). A better representation of zooplankton in the model would probably have given rise to deviating patterns (see below). A band of increased primary and export production is visible along the maximum extension of sea ice during the cold year 1981. During the warm year 1984 increases in carbon flux are more evenly distributed, covering large areas of the central and eastern Barents Sea (Fig. 7).

A comparison of primary production and vertical carbon flux during warm and cold years as based on 3-D simulations is difficult, in particular when data to validate the simulation results are limited and only available for some, but missing from most other areas. We therefore focus first on results from "Transect I" where adequate data coverage is available (Fig. 2). The nitrate consumption by phytoplankton in the warm year

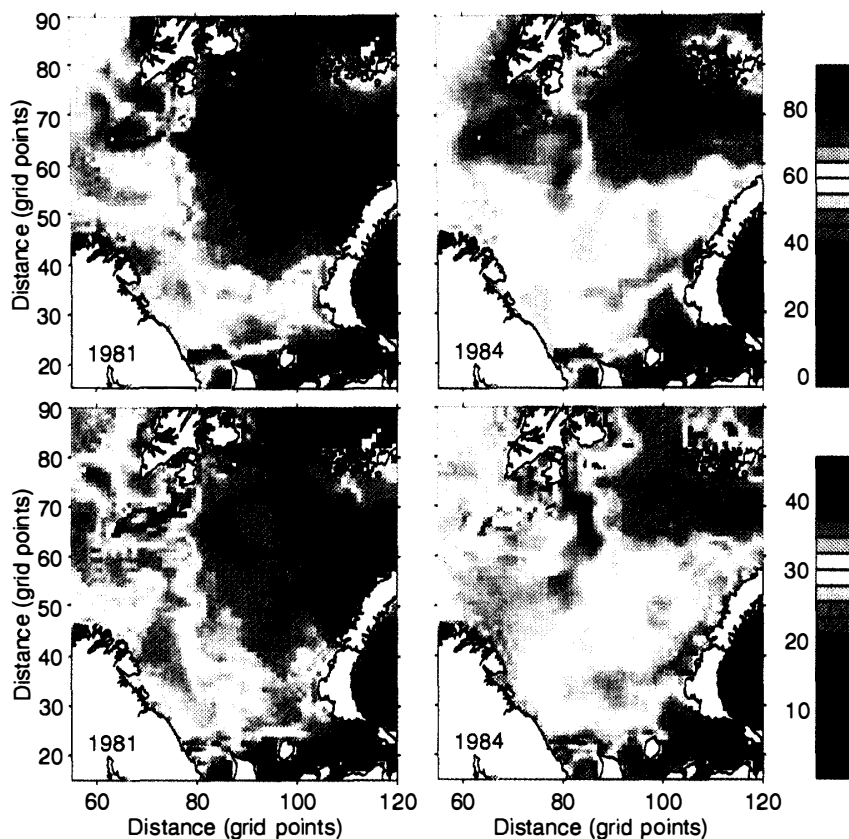


Fig. 7. Simulated annual primary production (above) and vertical export of phytoplankton derived carbon (below) at 75 m depth for the years 1981 and 1984 (mg C m^{-2}).

1984 was higher than that in the cold year 1981 (data not shown). Also the annual primary production along the transect in 1984 was far higher compared with that in 1981 (Fig. 8). In general, the annual primary production varied between about 40 to 90 g C m^{-2} . The greatest difference was found in the Atlantic water west for Central Bank, where the annual primary production was almost doubled in 1984 compared to 1981. In the southern and northern part of the transect the differences in annual primary production were probably of minor significance. This is also reflected in Fig. 9, showing the difference between the integrated annual primary production over the whole area of the cold and warm year. A long band of significantly increased primary production during warm years is observed along the coast of Novaya Zemlya and the Svalbard Bank. This is a direct consequence of the ice distribution during spring. In some areas, north-east of Novaya Zemlya and north of Franz Joseph Land, the annual primary production increases more than 4 times during warm years. This is caused by a continuous ice coverage during cold and partly open water during warm years, illustrating the great variability in primary production in areas where the ice is not receding every year. In an area off the coast of Norway and the Kola Peninsula the primary production was about 10% lower during the warm year. From 72°N and northwards the annual primary production in the entire Barents Sea was about 30% higher during 1984 compared to 1981.

Similar patterns were found for the export of phytoplankton derived carbon (Figs. 8

and 9). Vertical export of carbon was generally significantly higher during the warm year, in particular in the middle of the transect with the greatest variability in ice coverage (Fig. 8). In general, the annual vertical carbon export varied between about 17 to 39 g C m^{-2} . The greatest differences were found in the Atlantic water west for Central Bank, where the annual primary production was almost doubled in 1984 compared to 1981. In the southern and northern part of the transect the differences in annual primary production were probably of minor significance. The greatest variability in vertical carbon export as a function of climate change is supposed to be found along the coast of Novaya Zemlya, the Svalbard Bank, north-east of Novaya Zemlya and north of Franz Joseph Land.

The effect of ice coverage on the carbon flux in the Arctic has rarely been considered in most climate models. Ice may be either an accelerator (by changing albedos and transport patterns) or regulator (by insulation and latent heat of fusion) of climate change. In fact, little is known about even the direct response of ice covers to changes in atmospheric conditions (RAMSDEN and FLEMING, 1995). The Barents Sea obviously fixes up to 8 mole $\text{CO}_2 \text{ m}^{-2} \text{ y}^{-1}$ and exports to the aphotic zone as much as half of this, with an interannual variability of about 30%. However, the Barents Sea is relatively shallow and surface water is mixed during winter to depths greater than 100 m. POC and CO_2 accumulated at depth from the productive season is either redistributed, advected from the shelf to the adjacent Arctic Ocean or Norwegian Sea or released to the atmosphere. Most probably the Barents Sea does not contribute greatly to carbon storage in the Arctic which influences the atmospheric CO_2 concentration. In order to estimate the consequences for the carbon flux in the Barents Sea in a scenario of doubled atmospheric CO_2 concentrations only speculations can be presented. A coupled ice-ocean model revealed that if the atmospheric CO_2 concentrations was doubled, it appears that the Arctic ice cover would shrink in area and thickness, but would not disappear completely (RAMSDEN and FLEMING, 1995). The volume decrease in this work are in the order of 20%, whereas

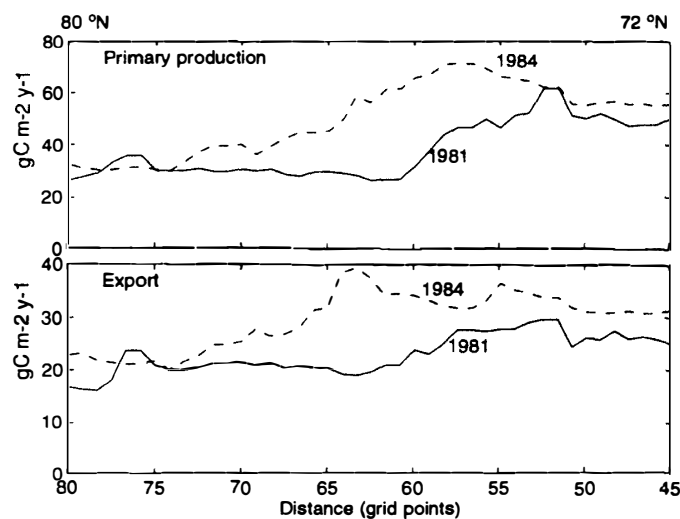


Fig. 8. Simulated annual primary production (above) and vertical carbon flux at 75 m depth (below) (g C m^{-2}) along "Transect I" for the years 1981 and 1984.

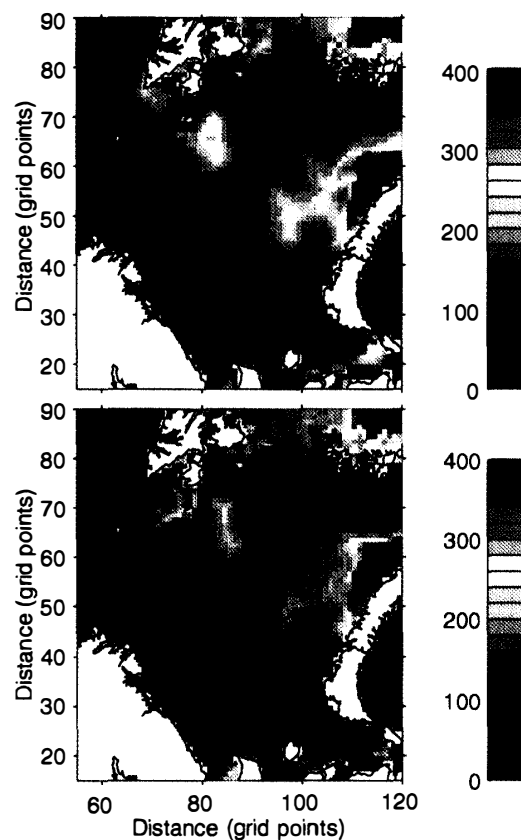


Fig. 9. Relative annual primary production (above) and vertical carbon flux at 75 m (below) in 1984 in percent of 1981. There are obvious increases in primary production and vertical carbon flux during warm years in the central Barents Sea, north-west of Novaya Zemlya and north of Franz Joseph Land, with some minor decreases in the southern and south-western part of the Barents Sea.

the decrease in area extent is in the order of 10% with significant open waters created only in the Kara and Beaufort Sea.

A doubling of the atmospheric CO₂ concentration would probably not only give rise to decreased ice cover, thinner ice, increased turbulent diffusion, increased nutrient consumption and primary production. It would also result in higher water temperature and changes in the plankton community. Major changes in the function of the Barents Sea ecosystem would most likely emerge. The mathematical representation of growth, respiration and sinking of organisms as presented in the present model may not be adequate any more under these conditions. Non-predictable biological changes in ecosystems caused by climate change limit the use of models for predictions of future carbon flux since changes cannot be extrapolated from current conditions.

4. General Remarks, Conclusion and Future Application

The carbon dynamics of large, remote ecosystems can rarely be understood on the base of field data alone due to incomplete coverage in space, depth and time. Whenever mathematical models are available in system ecological research, the dynamics of the dominating processes involved in carbon cycling should be studied by incorporating appropriate algorithms since this technique is often the only feasible approach to study in greater detail the carbon dynamics under a variety of environmental conditions. The most significant advantage of mathematical modelling is sensitivity testing of various compartments and processes. In this way modelling can guide the scientist to study in

greater detail those processes which give rise to the largest variability and which are least understood.

Given the lack of oceanographic data from the Arctic the only adequate method for the time being to address questions relating the role of the Arctic for climate change seems to be mathematical modelling based on available information on the meteorological, physical, chemical and biological oceanography of the area. The precision, accuracy and complexity of mathematical models can always be questioned and the present contribution is no exception. For example, meso-zooplankton grazing and production in the Barents Sea varies greatly from year to year (SKJOLDAL and REY, 1989; WASSMANN and SLAGSTAD, 1993). These are important processes for (a) the recycling of nutrients and biomass in the upper layers and vertical carbon export, (b) they change presumably along north-south and east-west gradients and (c) they are subjected to interannual and seasonal variation due to advection of CV and adult individuals from the Norwegian Sea (PEDERSEN, 1995). Also micro-zooplankton seems to play a far more important role in the Arctic than previously anticipated (*e.g.* ANTIA, 1991; HANSEN *et al.*, 1995). However, little is known about the annual dynamics of micro-zooplankton or the meso-zooplankton in the entire Barents Sea. The lack of sufficient knowledge regarding zooplankton in the entire Barents Sea results in that no adequate mathematical representation in the model can be accomplished at present. The simulation results are therefore run with a fixed meso-zooplankton module (see Material and Methods). The results reflect thus production and vertical carbon flux under the exclusion of variable zooplankton grazing. An adequate representation of zooplankton in future revisions of the present model will be of utmost significance in order to increase the realism of the simulations.

Despite this, we have no apparent doubts that the concentrations and main patterns of primary production and vertical carbon flux in space and time are represented clearly incorrect or inaccurate by the model. A validation of the simulation results with meteorological, oceanographic and biological data, in particular from Transect I, gave close fits. The presented scenarios primarily aim at to illustrate the dynamics of climatic forcing on the particulate carbon flux, not to deliver best possible approximations of rates over the entire area. For this reason, this contribution represents a first step to address quantitatively the 3-D dynamics of primary and vertical carbon flux in the Barents Sea until better models and, even more important, more extensive data sets from the entire Barents Sea are available.

As revealed by the model, the most important difference in carbon flux in the Barents Sea between cold and warm years are:

- The ice coverage during cold years is significantly larger. This is caused by the combined effects of (a) the heat capacity of the water, (b) the extent of the ice cover the previous year and (c) the dominating wind direction during the following winter.
- During cold years with extensive ice coverage large areas of the Barents Sea were subjected to marginal ice zone conditions with respect to vertical stability, giving rise to reduced vertical mixing and lower availability of nutrients. During summer the average temperature below the pycnocline was 0.5 – 2°C lower during cold compared to warm years.
- The primary production in the areas influenced by Atlantic water is significantly higher compared to those areas controlled by Arctic water. This is caused by that (a) radiation

is not reduced by the ice cover during spring and early summer and that (b) the insignificant vertical stability introduces nutrients to the upper layer. During cold years with an extensive ice cover, larger parts of the Barents Sea will experience arctic production conditions with significantly decreased primary production rates. The total annual primary production in the entire Barents Sea is 30% higher in warmer compared to colder years. In certain areas, however, deviations of more than 400% can be expected.

The ecological conditions in the Barents Sea are determined by the balance between (a) Atlantic and Arctic water, (b) the general meteorological conditions as reflected in the wind field and (c) the ice conditions in the previous year. The Barents Sea is thus not entirely a true part of the Arctic, but rather an area which balances between Atlantic and Arctic dominance in the south and north, respectively, and an extensive, climatically variable and often ice-covered intermediate area. Climate change will therefore be easily studied in the Barents Sea because of the delicate balance between Atlantic and Arctic water and the large extension and variation of the marginal ice zone. Major, general changes in climate change are presumably easy to detect due to the large variations in temperature, vertical stability, ice coverage and primary production.

We would like to present two examples for future application of the model. (1) The 3-D model presented here may be an important tool to investigate the consequences of climate change in the model area. Model simulations where extreme climatic scenarios are studied could be used to analyse the implicit consequences for and the interannual and interdecadal variability of the carbon flux. (2) The structure of long-lived macrobenthic communities can be used to study short-term variations in environmental conditions. In addition, the geological record as reflected by sediments is frequently used to scrutinise climate change. The simulation results presented here could be applied to identify areas in the model area where changes in carbon supply to the sediment, benthic growth and accumulation are expected to be greatest.

Acknowledgments

This investigation was supported by the Norwegian Research Council (NFR) and the working group of Petroleum Activities (AKUP). The hydrographical data were provided by the Institute of Marine Research, Bergen. A special thank to Harald LOENG for helpful discussions during the work. This is a contribution from the research programme North Norwegian Coastal Ecology (MARE NOR).

References

- ÅDLANDSVIK, B. and LOENG, H. (1991): A study of the climatic system in the Barents Sea. *Polar Res.*, **10**, 45–49.
- ANDERSON, L.G., DYRSSEN, D. and JONES, E.P. (1990): An assessment of the transport of atmospheric CO₂ into the Arctic Ocean. *J. Geophys. Res.*, **95**, 1703–1711.
- ANTIA, A.V. (1991): Micro-zooplankton in the pelagic food web of the east Greenland Sea and its role in sedimentation processes. *Ber Sonderforschungsbereich 313 Univ. Kiel*, **33**, 1–109.
- BÅMSTEDT, U., EILERTSEN, H.C., TANDE, K., SLAGSTAD, D. and SKJOLDAL, H.R. (1991): Copepod grazing and its potential impact on the phytoplankton development in the Barents Sea. *Polar Res.*, **10**, 339–353.

- BIRD, R.E. (1983): A simple, solar spectral model for direct-normal and diffuse horizontal irradiance. *Sol. Energy*, **32**, 461–471.
- BROECKER, W.S. and PENG, T.H. (1990): The cause of the glacial to interglacial atmospheric CO₂ change: Polar alkalinity hypothesis. *Global Biogeochem. Cycles*, **3**, 215–239.
- GOULD, W.J., LOYNES, J. and BACKHAUS, J. (1985): Seasonality in slope current transport NW of Shetland. ICES Paper C.M. 1985/C:7.
- HANSEN, B., CHRISTIANSEN, S. and PEDERSEN, G. (1995): Plankton dynamics in the marginal ice zone of the central Barents Sea during spring: Carbon flow and structure of the grazer food chain. submitted to *Polar Biol.*
- HARMS, I. (1994): Numerische Modellstudie zur winterlichen Wassermassen-formation in der Barentssee. Ph. D. Thesis. Institut für Meereskunde. Hamburg.
- HASSELMANN, K., BARNETT, T.P., BOUWS, E., CARSLON, H., CARTWEIGHT, D.E., ENKE, K., MEERBURG, A., MÜLLER, P., OLBERS, D.J., RICHTER, K., SELL, W. and WALDEN, H. (1973): Measurements of Wind-Wave Growth and Swell Decay during the Joint North Sea Wave Project (JONSWAP). *Deutsche Hydrographische Zeitschrift, Reihe A* (80), No. 12, 95 p.
- HIBLER III, W.D. (1979): A dynamic thermodynamic sea ice model. *J. Phys. Oceanogr.*, **9**, 815–846.
- ICHIYE, T. (1967): Upper ocean boundary-layer flow determined by dye diffusion. *Phys. Fluids Suppl.*, **10**, 270–277.
- IVERSON, R. (1990): Control of fish production. *Limnol. Oceanogr.*, **35**, 1593–1604.
- KIRK, J.T.O. (1983): *Light and Photosynthesis in Aquatic Ecosystems*. Cambridge, Cambridge Univ. Press, 404 p.
- LEGENBRE, L. (1990): The significance of microalgal blooms for fisheries and for the export of particulate organic carbon in the ocean. *J. Plankton Res.*, **12**, 681–699.
- LODER, J.W. and GREENBERG, D.A. (1986): Predicted positions of tidal fronts in the Gulf of Maine region. *Cont. Shelf Res.*, **6**, 397–414.
- LOENG, H. (1987): The effect of oceanographic conditions on distribution and population dynamics of commercial fish stocks in the Barents Sea. *The Effect of Oceanographic Conditions on Distribution and Population Dynamics of Commercial Fish Stocks in the Barents Sea; Proc 3rd Soviet-Norwegian Symposium*, ed. by H. LOENG. Bergen, Inst. Mar Res., 1–250.
- LOENG, H. (1991): Features of the physical oceanographic conditions of the Barents Sea. *Polar Res.*, **10**, 5–18.
- LØYNING, T.B. and VINJE, T. (1991): The effect of ice concentration on the wind drift of sea ice and icebergs. MOMOP Report. Oslo, Norskpolarinstitutt, 26 p.
- MARTINSEN, E. and ENGEDAHL, H. (1987): Implementation and testing of a lateral boundary scheme as an open boundary condition in a barotropic ocean model. *Coastal Eng.*, **11**, 603–627.
- MCCCLIMANS, T.A. (1993): An algorithm for computing monthly averaged inflow of Atlantic water to the Norwegian Sea. SINTEF Report. STF60 A93009.
- MCCCLIMANS, T.A. and NILSEN, J.H. (1990): A laboratory simulation of the ocean currents of the Barents Sea during 1979–1984. SINTEF NHL Report STF60 A90018. Trondheim.
- MESINGER, F. and ARAKAWA, A. (1976): Numerical methods used in atmospheric models. *GARP Publ. Ser. WMO*, **17**, 64 p.
- MIDTTUN, L. and LOENG, H. (1987): Climatic variations in the Barents Sea. *The Effect of Oceanographic Conditions on Distribution and Population Dynamics of Commercial Fish Stocks in the Barents Sea; Proc 3rd Soviet-Norwegian Symposium*, ed. by H. LOENG. Bergen, Inst. Mar Res., 13–27.
- MYSAK, L. and SCHOTT, F. (1977): Evidence for baroclinic instability of the Norwegian Current. *J. Geophys. Res.*, **82**, 2087–2095.
- PARSONS, T.R., TAKAHASHI, M. and HARGRAVE, B. (1983): *Biological Oceanographic Processes*. Oxford, Pergamon Press, 332 p.
- PEDERSEN, G. (1995): Factors influencing the size and distribution of the copepod community in the Barents Sea with special emphasis on *Calanus finmarchicus* (Gunnerus). Dr. Sci. Thesis, University of Tromsø, Norway.
- PRICE, J.F. and WELLER, A. (1986): Observations and models of the upper ocean response to diurnal heating, cooling, and wind mixing. *J. Geophys. Res.*, **91**, 8411–8427.

- RAMSDEN, D. and FLEMING, G. (1995): Use of a coupled ice-ocean model to investigate the sensitivity of the Arctic ice cover to doubling atmospheric CO₂. *J. Geophys. Res.*, **100**, 6817–6828.
- REY, F., SKJOLDAL, H.R. and SLAGSTAD, D. (1987): Primary production in relation to climatic changes in the Barents Sea. The Effect of Oceanographic Conditions on Distribution and Population Dynamics of Commercial Fish Stocks in the Barents Sea; Proc 3rd Soviet-Norwegian Symposium, ed. by H. LOENG. Bergen, Inst. Mar Res., 29–46.
- SAKSHAUG, E. and SKJOLDAL, H.R. (1989): Life at the ice edge. *Ambio*, **18**, 60–67.
- SAKSHAUG, E., HOPKINS, C.C.E. and ØRITSLAND, N.A., ed. (1991): Proceedings of the Pro Mare Symposium on Polar Marine Ecology, Trondheim, Norway, 12–16 May 1990. *Polar Res.*, **10**, 1–662.
- SAKSHAUG, E., REY, F. and SLAGSTAD, D. (1995): Wind forcing of marine primary production in the Northern atmospheric low-pressure belt. *Ecology of Fjords and Coastal Waters*, ed. by H.R. SKJOLDAL *et al.* Amsterdam, Elsevier, 15–25.
- SARMIENTO, J.L. and TOGGWEILER J.R. (1984): A new model for the role of the oceans in determining atmospheric P_{CO₂}. *Nature*, **308**, 621–624.
- SKJOLDAL, H.R. and REY, F. (1989): Pelagic production and variability of the Barents Sea ecosystem. *Biomass and Geography of Large Marine Ecosystems*, ed. by K. SHERMAN and K.L. ALEXANDER. Boulder, Westview Press, 243–283.
- SKJOLDAL, H.R., HASSEL, A., REY, F. and LOENG, H. (1987): Spring phytoplankton development and zooplankton reproduction in the central Barents Sea in the period 1979–1984. The Effect of Oceanographic Conditions on Distribution and Population Dynamics of Commercial Fish Stocks in the Barents Sea; Proc 3rd Soviet-Norwegian Symposium, ed. by H. LOENG. Bergen, Inst. Mar Res., 59–90.
- SLAGSTAD, D. (1987): A 4-dimensional physical model of the Barents Sea. SINTEF report STF48 F87013, 1–34.
- SLAGSTAD, D. and STOKKE, S. (1994): Simulation of flow field, hydrography, ice cover and primary production in the Northern Barents Sea. *Fisken Havet*, **9**, 47 p. (in Norwegian).
- SLAGSTAD, D. and STØLE-HANSEN, K. (1991): Dynamics of plankton growth in the Barents Sea. *Polar Res.*, **10**, 173–186.
- SLAGSTAD, D., STØLE-HANSEN, K. and LOENG, H. (1989): Density driven currents in the Barents Sea calculated by a numerical model. *Modelling, Identification and Control*, **11**, 181–190.
- STØLE-HANSEN, K. and SLAGSTAD, D. (1991): Simulation of currents, ice-melting and vertical mixing in the Barents Sea using a 3-D baroclinic model. *Polar Res.*, **10**, 33–44.
- STØLE-HANSEN, K., SLAGSTAD, D. and UTNES, T. (1989): Baroclinic Model Test Case Information. SINTEF report STF48 F89002. Trondheim.
- TANDE, K.S. (1991): Calanus in high latitude environments. *Polar Res.*, **10**, 389–407
- TINGELE, A., DIETERLE, D. A. and WALSH, J. J. (1979): Perturbation analysis of the New York Bight. *Ecological Process in Coastal and Marine Systems*, ed. by R.J. LIVINGSTON. New York, Plenum Press, 395–435.
- VINJE, T. and KVAMBEKK, Å.S. (1991): Barents Sea drift ice characteristics. *Polar Res.*, **10**, 59–68.
- WASSMANN, P. and SLAGSTAD, D. (1993): Seasonal and interannual dynamics of carbon flux in the Barents Sea: A model approach. *Polar Res.*, **13**, 363–372.
- WASSMANN, P., PEINERT, R. and SMETACEK, V. (1991): Patterns of production and sedimentation in the boreal and polar north-east Atlantic. *Polar Res.*, **10**, 209–228
- WORTHINGTON, L.V. (1970): The Norwegian Sea as a Mediterranean sea. *Deep-Sea Res.*, **17**, 77–84.
- ZUBOV, N.N. (1945): *L'dy Arktiki*. Moscow, Izdatel'stvo Glavsevmorputi, 360 p. (in Russian).

(Received November 10, 1995; Revised manuscript accepted May 20, 1996)